

Microbial size spectra from natural and nutrient enriched ecosystems

Kent K. Cavender-Bares¹

Ralph M. Parsons Laboratory, Department of Civil and Environmental Engineering, 48-425, Massachusetts Institute of Technology, Cambridge, Massachusetts 02139

Andrea Rinaldo

Ralph M. Parsons Laboratory, Department of Civil and Environmental Engineering, 48-425, Massachusetts Institute of Technology, Cambridge, Massachusetts 02139; and Dipartimento di Ingegneria Idraulica, Marittima e Geotecnica, Università di Padova, via Loredan 20, I-35131 Padova, Italy

Sallie W. Chisholm²

Ralph M. Parsons Laboratory, Department of Civil and Environmental Engineering, and Department of Biology, 48-425, Massachusetts Institute of Technology, Cambridge, Massachusetts 02139

Abstract

Microbial size spectra, including bacteria through nanophytoplankton, were measured by use of flow cytometry across the western north Atlantic Ocean and during two nutrient enrichment studies: bottle enrichments in the Sargasso Sea and an in situ iron enrichment in the equatorial Pacific (IronEx II). Spectral shapes, or the relative conformity to a function described by a power law, ranged from smooth and log linear during the spring bloom in the Sargasso Sea to being distinctly non-log linear in coastal waters. Overall, the individual spectra within large regions characterized by similar ecological conditions showed remarkable consistency, inviting speculation that powerful organizing mechanisms are at work in these communities. Moreover, the ensemble average of all of the spectra along the transect displays clear power-law behavior. Slopes ranged from -1.0 , in which biomass was equally distributed between all size classes, to -1.4 , in which proportionally more biomass was contained in smaller size classes; there was no clear relationship between nutrient concentrations and spectral slopes over the entire data set. Species succession in nutrient-enriched bottles caused spectra to evolve from relatively smooth power laws to distributions showing preferred sizes (i.e., nonlinear on a log-log plot). The IronEx II spectra, however, remained similar over the course of the experiment. It could be that the elimination of bottle effects in this experiment buffered the system in ways that maintained the size structure of the microbial community over the size range we measured. Our results suggest conditions that lead to log-linear size distributions; these should be verified over a broader range of scales and environments.

Size spectra, which display the relative abundance of organisms of different sizes, convey a synoptic image of ecological communities that is taxon independent. As such, they have been attractive to ecological theorists and have been the subject of periodic interest in marine ecology for the past 30 yr. Sheldon et al. (1972, 1977) recognized the predictive powers of size spectra, suggesting that fish stocks could be predicted if the planktonic size spectrum were known. Moreover, a spectral approach offers potential for enhancing ecosystem models (Gin et al. 1998), including those that focus

on ocean biogeochemistry (Armstrong 1999). In addition, Stramski and Kiefer (1991) have demonstrated the utility of a spectral approach for interpreting ocean color measurements from satellites.

Considerable attention has been paid to the details of representing size spectra and the theoretical underpinnings thereof (see Platt 1985; Blanco et al. 1994; Vidondo et al. 1997). Platt and Denman's (1978) normalized biomass spectrum has been the model employed most often for representing the spectra of planktonic organisms. In idealized form, it fits a linear model on a double logarithmic plot (i.e., a power law, or algebraic decay) of normalized biomass versus particle size. When the slope of the log-transformed spectrum is -1.0 , there is an even distribution of biomass among all size classes—the situation observed by Sheldon and co-workers (Sheldon et al. 1972, 1977)—that has invited explanation for some time (e.g., Platt and Denman 1978; Kiefer and Berwald 1992). Many studies have shown that, regardless of slope, a log-linear model appropriately characterizes planktonic spectra (e.g., Rodriguez and Mullin 1986; Ahrens and Peters 1991), although not equally well in all situations (e.g., Sprules et al. 1983; Tittel et al. 1998). Rodriguez and Mullin (1986) argued that the significance of power-law descriptions of size spectra per se may be of more value than a detailed analysis of slopes.

¹ Present address: The H. John Heinz III Center for Science, Economics and the Environment, 1001 Pennsylvania Ave., NW Suite 735 South, Washington, DC 20004.

² Corresponding author (chisholm@mit.edu).

Acknowledgements

We thank the captain and crew of the R/V *Oceanus*, who facilitated the collection of the transect data through challenging weather conditions. We thank M. Durand and R. Greene for help developing the Mie fit to our calibration data. We also thank R. Olson and L. Moore for helpful comments on earlier drafts of this manuscript and J. Rodríguez and an anonymous reviewer for valuable critical comments. This work was supported in part by the U.S. National Science Foundation (grant OCE-9302529), MIT/TEPCO funds, and the MIT Joint Program in the Science and Policy of Global Change.

Power laws are ubiquitous in nature. They have been shown to describe many objects, from coastlines, clouds, or mountain profiles (Mandelbrot 1983) to networks like rivers or, recently, the worldwide web (Albert et al. 2000). Distributions of random variables that follow power laws are scale free, and as such they are extremely inhomogeneous. This is best visualized through a network model constituted by nodes and links. If the network follows a power law, most nodes have one or two links, and a few nodes will have a large number of links and play a key role in the behavior of the network (Barabasi and Albert 1999). Size distributions are derived from a network of interactions (i.e., the food web), and, thus, the emergence of power laws in these distributions could bear fundamental ecological implications. Conversely, deviations from power laws also prompt important questions, for they indicate the presence of characteristic sizes (Schroeder 1991), which are affected by how ecological processes structure ecosystems across scales in time and space (Holling 1992).

Historically, several measurement techniques have been used to construct planktonic size spectra, each of which represents a compromise. Sheldon and coworkers (e.g., Sheldon and Parsons 1967; Sheldon et al. 1972) used the Coulter Counter, which cannot distinguish between intact cells and detritus. Subsequent studies have relied on microscopy to characterize microorganisms, to eliminate the bias resulting from the inclusion of detrital particles (e.g., Rodriguez and Mullin 1986; Ahrens and Peters 1991; Gaedke 1992; Ruiz et al. 1996; Tittel et al. 1998). This greatly improves the quality of the data, but the labor-intensive nature limits the number of data points, thus limiting resolution on the size axis. After some initial trials showing that flow cytometry might be a useful tool for creating high-resolution phytoplankton size spectra (Yentsch and Phinney 1989; Chisholm 1992), Li (1994) presented the first detailed analysis of microbial spectra in the north Atlantic. This technology, which is capable of characterizing phytoplankton and bacteria, has the advantage of being able to analyze tens to hundreds of cells per second. It has the disadvantage of being able to analyze only a relatively narrow range of cell sizes. In Li's (1994) pioneering study, forward-angle light scatter (FALS) was used directly as a proxy for cell volume. Although the two are related in phytoplankton (e.g., Olson et al. 1989), the relationship is not constant over all size classes (e.g., Ackelson and Spinrad 1988; Gin 1996). More recent studies have tried to correct for this (Gin 1996; Gin et al. 1999), albeit still imperfectly, by calibrating the FALS signal with use of laboratory cultures and field populations that have been filter fractionated. We build on the methodology of Gin et al. (1999) in this work by using a refined relationship between FALS and cell size derived directly from field populations of marine phytoplankton (Cavender-Bares 1999). In addition, we eliminated error due to preservation of large cells (Lepesteur et al. 1993) by analyzing them fresh. Finally, we represent spectra as probabilities of exceedence, eliminating the need for binning data and that procedure's inherent problems (Vidondo et al. 1997).

The goal of this study was to use this improved methodology to measure microbial size spectra at high frequencies along a transect encompassing diverse ecological conditions

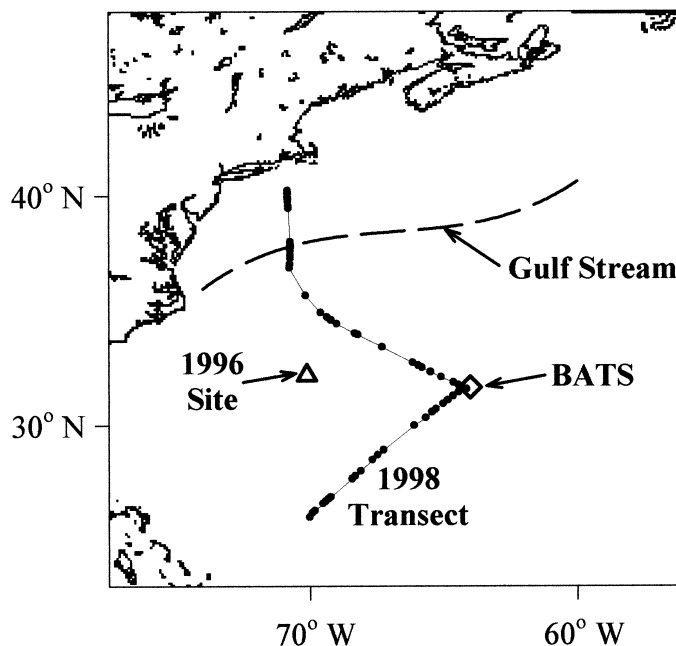


Fig. 1. Map of sampling stations in the western Atlantic Ocean during March 1998. The approximate location of the Gulf Stream is shown by a dashed line, and the BATS site is denoted by a diamond. A triangle represents the site of an enrichment experiment conducted during June 1996.

and to compare these patterns with those observed in experimentally perturbed ecosystems. We were interested in determining (1) over what spatial or ecological scales the spectral properties would be highly conserved and whether these properties could be associated with specific ecosystem characteristics; (2) under what conditions the spectra would obey power laws; (3) under what conditions—if any—the spectra would display a slope of -1.0 , indicating an even distribution of biomass among size classes; and (4) whether we could distinguish the effect of partial and whole ecosystem perturbations. Specifically, we examined size spectra along a detailed transect across the Sargasso Sea, the Gulf Stream, and coastal waters of the western north Atlantic Ocean. We then compared the spectral patterns revealed during this observational study with those derived from two experimental nutrient enrichment studies: manipulations in bottles at a site in the oligotrophic Sargasso Sea and an *in situ* iron-fertilization experiment in the high-nutrient, low-chlorophyll region of the equatorial Pacific Ocean (IronEx II; Coale et al. 1996). We were motivated by the belief that measuring spectra under this diverse set of circumstances might help resolve the constant and variable features of foodweb structure in these ecosystems and provide data for future theoretical treatments.

Methods

Atlantic transect—Measurements of biological and chemical features were made along a transect in the Atlantic during March 1998 (Fig. 1). In all cases, samples were drawn

from the ship's laboratory seawater system, the inlet of which was nominally at a depth of 3 m.

Enrichment experiments—An enrichment study was conducted in bottles at an oligotrophic station in the Sargasso Sea during June 1996 (Fig. 1), where ambient nutrient concentrations were well below 10 nM for both nitrate + nitrite (N+N) and soluble reactive phosphorus (SRP; Cavender-Bares 1999). Water was collected from 20 m by use of an acid-washed Go-Flo bottle suspended on a Kevlar line and was dispensed into triplicate bottles for both control and treatments; 80 μM NO_3^- and 5 μM PO_4^{3-} were added to treated bottles as NaNO_3 and NaH_2PO_4 , respectively. Bottles were placed within an incubator on the ship's deck, in which temperature was maintained by flowing seawater, and ambient light was attenuated with neutral density screening in order to approximate the light level at 20 m.

We also monitored changes in size spectra during the second in situ iron-fertilization experiment in the equatorial Pacific Ocean (IronEx II; Coale et al. 1996). Briefly, three separate infusions of iron [added as Fe(II) in seawater at pH 2] were made into a region of surface water measuring 72 km^2 during May and June of 1995. Initial nitrate concentrations were high ($\sim 10 \mu\text{M}$), as were initial concentrations of phosphate ($>0.5 \mu\text{M}$; Coale pers. comm.), whereas initial Fe(II) concentrations were only 0.05 nM (Coale et al. 1996).

Measurement of chlorophyll and nutrients—Chlorophyll *a* (Chl *a*) was analyzed following the acid-correction method (June 1996 samples) or Welschmeyer (1994) method, which eliminates the need for a pheophytin correction. Analyses were done at sea (June 1996) or on GF/F filters (Whatman) that had been frozen in liquid nitrogen. N+N and SRP were analyzed by use of Garside's (1982) chemiluminescence method and Karl and Tien's (1992) magnesium-induced coprecipitation (MAGIC) method, respectively (see Cavender-Bares 1999; Cavender-Bares et al. in press). A concurrent study described similar SRP concentrations for a portion of the same transect (Wu et al. 2000). Detection limits for N+N measured by chemiluminescence were ~ 2 nM, and those for SRP were ~ 0.5 nM.

Collection of size-structured data—A modified Epics V flow cytometer (Beckman-Coulter) was used both at sea and in the laboratory for all plankton analyses (Cavender-Bares et al. 1998, 1999). Four groups of plankton were distinguished by these analyses. Bacteria were enumerated by staining samples with a nucleic acid-specific stain (SYBR-Green I, Molecular Probes), following the protocol of Marie et al. (1997). These samples had been preserved with use of 0.1% glutaraldehyde and were frozen in liquid nitrogen. *Prochlorococcus* and *Synechococcus* were analyzed either at sea or on similarly preserved but unstained samples. It has been our experience that the flow cytometric characteristics of the larger phytoplankton, which have been classified as the ultra- and nanoplankton (Cavender-Bares et al. 1999), are not well preserved (Lepesteur et al. 1993; Gin 1996). Thus, this fraction of the community was analyzed in fresh samples at sea.

We applied a calibration curve (Fig. 2) to the raw flow

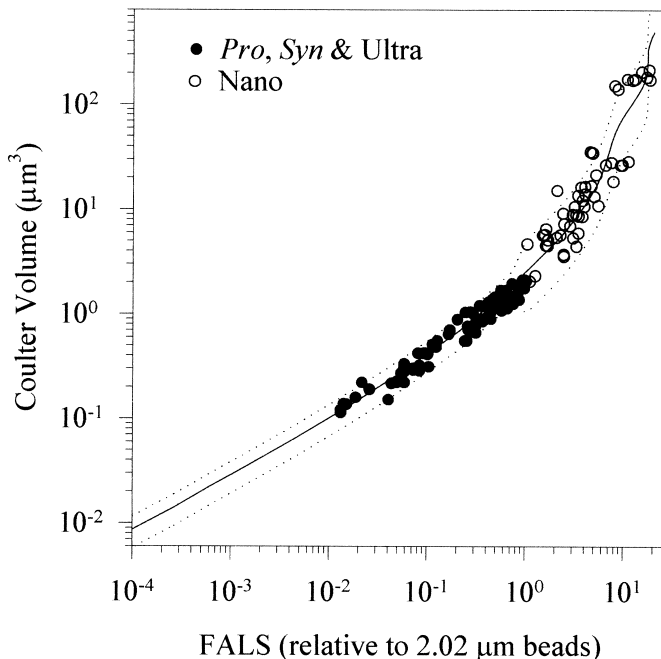


Fig. 2. Calibration curve used to convert FALS to equivalent spherical volume as measured by a Coulter Counter. Two groups of phytoplankton are shown: filled circles for *Prochlorococcus*, *Synechococcus*, and the ultraphytoplankton and open circles for the nanophytoplankton. The solid line is calculated from Mie theory (see text), and dotted lines represent estimated confidence limits for predicting volume from FALS. Note that FALS values are reported relative to the FALS of standard calibration beads.

cytometry data in order to convert from FALS to cell volume. The development of this calibration curve is described elsewhere (Cavender-Bares 1999). In brief, each data point resulted from sorting (via flow cytometry) a subset of cells in a preserved field sample away from the others and then sizing those cells with use of a Coulter Counter (Model ZM, Beckman-Coulter; see Cavender-Bares 1999). A fit to the data based on the equations of Bohren and Huffman (1983) for Mie theory, which is similar to the modeling done by Ackelson and Spinrad (1988), is shown in Fig. 2, along with dotted lines representing our estimate of 95% confidence intervals on predicting volume from FALS. The points at low FALS correspond to populations of *Prochlorococcus*. Instrument limitations did not permit the sorting and sizing of bacteria; however, the slope of the Mie fit to the data extrapolated in this region agrees with work relating FALS to volume of marine bacteria (Robertson et al. 1998). Note that, because the lack of a smooth relationship in the Mie fit above a FALS of ~ 10 units ($\sim 5 \mu\text{m}$ diameter), we did not include cells of this FALS or greater in our size spectra. Note also that, because of their long, slender shape, the FALS-to-volume relationship for pennate diatoms is different than that for the rest of the ultra- and nanoplankton (Olson et al. 1989). This was only an issue for the IronEx II samples. Our calibration studies (Cavender-Bares 1999) indicated that the Coulter volume of these pennate diatoms was constrained to a fairly narrow range, centered at a volume of $10 \mu\text{m}^3$ (range 7–16 μm^3).

Although flow cytometry is a useful tool for generating highly resolved and statistically significant abundance versus size data, it is typically constrained to analyses of the small end of the phytoplankton size spectrum. Although most of the oceanographic provinces we examined are indeed dominated by very small cells, our study is still limited in that we were unable to examine cells larger than $\sim 5 \mu\text{m}$ as a part of our spectral analysis. Our hope is that broad-range flow cytometers will soon be developed to overcome these shortcomings.

On representing size spectra—Over the past 30 yr, there has been a considerable evolution in the methods of measuring and representing planktonic size spectra. Sheldon and Parsons (1967) presented their spectra as particle concentration (by volume) versus log(base 2) of particle diameter. This was replaced by Platt and Denman's (1978) normalized biomass spectrum (e.g., Rodriguez and Mullin 1986; Ahrens and Peters 1991; Ruiz et al. 1996; Tittel et al. 1998), which has some limitations (Prothero 1986; Blanco et al. 1994). More recently, the use of normalized cell concentration spectra has been recommended as a way to avoid these limitations (Blanco et al. 1994).

Because of the advent of instruments capable of measuring highly-resolved size spectra, Vidondo et al. (1997) proposed representing plankton spectra as probabilities of exceedence—an approach that has widely recognized utility for other applications in oceanography (e.g., Bader 1970; Stramski and Kiefer 1991) and in other disciplines (*see* references in Vidondo et al. 1997). When this approach is used, data need not be binned into size classes, avoiding the problems associated with binning (Blanco et al. 1994). Vidondo et al. (1997) propose fitting such spectra with either a linear fit on a log-log plot (Pareto I) or a more complex relationship that can be fitted to data sets with deviations from log linearity at small size (Pareto II).

We represent our spectra as $\log \text{Prob}(V \geq v)$ versus $\log v$ plots, in which $\text{Prob}(V \geq v)$ is the probability that a particle of random volume, V , is greater than or equal to a given volume, v . Practically, one measures the relative fraction, or frequency, of cells within a sample that are equal to or larger than a given volume, v . A slope (β) of -1 on such a log-log plot indicates that particle abundance is inversely proportional to particle size and that total biovolume is constant within arbitrarily equal size classes. As β becomes more negative, yielding steeper spectra (e.g., $\beta = -1.2$), proportionally more biovolume is distributed in small size classes; the opposite is true as β becomes more positive, or flatter.

In some cases, we present ensemble averages of size spectra in order to describe variability within a group of spectra. In such cases, it was assumed that all of the different spectra, or realizations, belonged to the same statistical population. Depending on the number of spectra averaged together, we used vertical error bars that either represent \pm range or ± 1 SD.

As was discussed in the previous section, the largest cells we measured were, in some cases, omitted from our spectra because of our uncertainty of their size, based on the nature of the calibration curve in that region (Fig. 2). However, it was confirmed that this truncation did not have an impact

on the features—specifically β values and spectral shapes—of the $\text{Prob}(V \geq v)$ curves (data not shown).

Results and discussion

North Atlantic transect

Chemical and biological features along transect—Surface temperature declined gradually from a high of 25°C at the transect's southernmost stations until deeply mixed waters were reached just south of the Bermuda Atlantic Time-series (BATS), at which point water temperatures remained at $\sim 19^\circ\text{C}$ northward until the warm (23°C) waters of the Gulf Stream were encountered (Fig. 3A). The northern edge of the Gulf Stream was well defined by an abrupt drop in temperature from 20°C to $\sim 10^\circ\text{C}$, followed by 5°C temperatures further northward. Chl a levels at the southernmost stations were low, ranging from 0.06 to $0.1 \mu\text{g L}^{-1}$. They increased about fourfold just south of BATS (range 0.3 – $0.6 \mu\text{g mL}^{-1}$), to reach a mean of $0.4 \mu\text{g L}^{-1}$ (Fig. 3A), which is characteristic of the spring bloom at BATS (Michaels et al. 1994). For the remainder of the north-west transect across the Gulf Stream, Chl a remained at these levels; values $>1 \mu\text{g L}^{-1}$ were seen in coastal waters.

Both N+N and SRP were <10 nM in the southern portion of the transect (Fig. 3B). The low SRP values, which had not been measured prior to this cruise (Wu et al. 2000; Cavender-Bares et al. in press), have been hypothesized to result from differential rates of remineralization of dissolved organic N and P (Wu et al. 2000). Moving northward, N+N increased nearly 100-fold just before reaching the BATS site, whereas SRP increased only ~ 10 -fold. The disparity between the increases of these two nutrient pools caused their N:P ratio to change from $<16:1$ in the southern Sargasso to a mean of $50:1$ in the north (Fig. 3C). The ratio dropped to $25:1$ in the Gulf Stream and to $<16:1$ in coastal waters. Ratios $<16:1$ in the southern Sargasso suggest that new production there was nitrogen limited (Dugdale and Goering 1967), whereas the elevated ratios in the northern Sargasso suggest that new production there was limited by phosphorus—if it was limited at all. It has been suggested that these elevated ratios result from remineralization of nitrogen-fixing cells, which are rich in N relative to P (Fanning 1992; Michaels et al. 1994). For this to be possible, growth would have to be favorable for nitrogen-fixing cells (i.e., N-limiting conditions, implying N:P ratios $<16:1$), which has recently been shown in general for stratified periods in the Sargasso Sea (Cavender-Bares et al. in press).

Patterns of size spectral features along transect

Spectral shape: In examining allometric phenomena in ecology, one can either focus on the differences or similarities, depending on one's point of view (Chisholm 1992). When we first looked at the family of spectra from the transect (Fig. 4), we were struck by both. Taken as a whole, and given the diversity of environments, the spectra along the entire transect are remarkably similar, for this size range at least, suggesting some self-organizing principle at work (Bak 1996). Looking more closely, the features of the individual

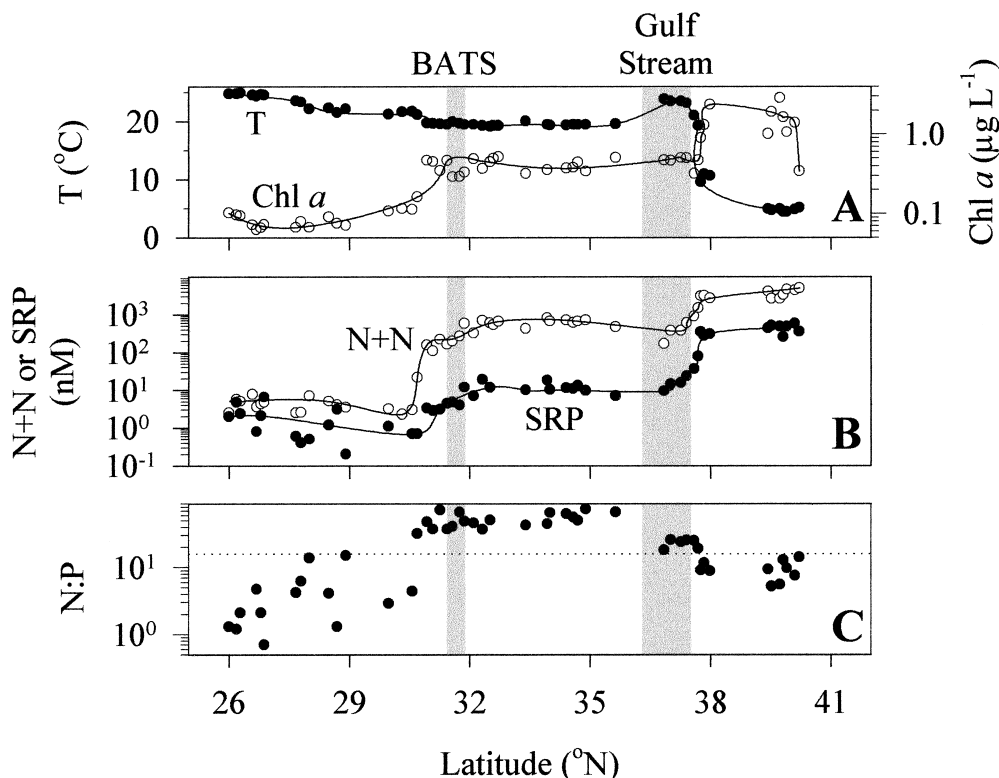


Fig. 3. Physical, chemical, and biological features along a transect (Fig. 1) from south of Bermuda in the Sargasso Sea across the Gulf Stream and into coastal waters. (A) Temperature and Chl *a*, (B) N+N and SRP, and (C) N+N:SRP along the transect, with a dotted line included at a ratio of 16:1 representing the Redfield ratio (adapted from Cavender-Bares et al. in press). Shaded regions represent the approximate location of BATS and the Gulf Stream.

spectra are nearly identical within regions that have similar ecosystem descriptors (e.g., Chl *a*, temperature, and nutrients), but they do change distinctly in shape moving from one regime to another. In particular, we saw distinct transitions between the southern and northern Sargasso Sea, in which nutrients changed significantly, and between the Gulf Stream and coastal waters. The ensemble averages (*see* Methods) of the individual spectra for each region (Fig. 5A–D), collapse into a single spectrum with small vertical error bars, which indicates very little variation within these regions and points toward meaningful scales of variability for the food webs within the different regions.

Several points of interest result from a qualitative inspection of the Prob($V \geq v$) spectra along the transect (Fig. 4). Prior to reaching the higher nutrient waters of the spring bloom just south of BATS (Fig. 3), spectra were remarkably similar, with a predominant nonlinearity (on the log-log scale), or waviness, located approximately at the center of the individual spectra (i.e., a flattening centered at a volume of $0.4 \mu\text{m}^3$; Fig. 4A). This flattening disappeared at the southern extent of the spring bloom (denoted by an asterisk in Fig. 4B), resulting in a more or less log-linear shape, which persisted north across the Gulf Stream. When the continental shelf was reached, deviations from linearity set in again but at a different position in the spectrum (Fig. 4C).

As is obvious from the individual spectra, the ensemble average of the 17 spectra from the southern region of the

transect (Fig. 5A) is characterized by a distinct flattening in the spectrum centered at $\sim 0.4 \mu\text{m}^3$ (diameter of $0.9 \mu\text{m}$)—reflecting an overrepresentation of cells in size classes from 0.1 to $0.4 \mu\text{m}^3$ and underrepresentation of cells in size classes from 0.4 to $2 \mu\text{m}^3$. A similarly wavy Prob($V \geq v$) curve, which is related to gaps in the size frequency distribution (Fig. 5H), was seen in the coastal region (Fig. 5D), with size classes in the range of 0.03 – 0.1 and 1 – $2 \mu\text{m}^3$ overrepresented and those in the range of 0.1 – $1 \mu\text{m}^3$ underrepresented; the flattening of the probability of exceedence curve that resulted was centered at $0.2 \mu\text{m}^3$ (diameter of $0.7 \mu\text{m}$). The spectra from the northern portion of the Sargasso Sea (Fig. 5B) and the Gulf Stream (Fig. 5C) were much more log linear, thereby closely conforming to a power law, indicating an algebraic decrease in cell number with increasing cell size.

By comparing the ensemble spectra (Fig. 5A–D) with the raw data used in their construction (Fig. 5E–H), their shapes can be understood in terms of the relative abundance of the several groups that are resolvable within the microbial community. The nearly flat region of the spectra in the southern Sargasso Sea (Fig. 5A) is due to a gap between *Synechococcus* and ultra- and nanoplankton populations (arrow in Fig. 5E), which is not evident in the northern Sargasso (Fig. 5F) and Gulf Stream (Fig. 5G). The populations filling this gap in the latter two regimes, however, are different. In the northern Sargasso, it is filled by a subpopulation in the ultra-

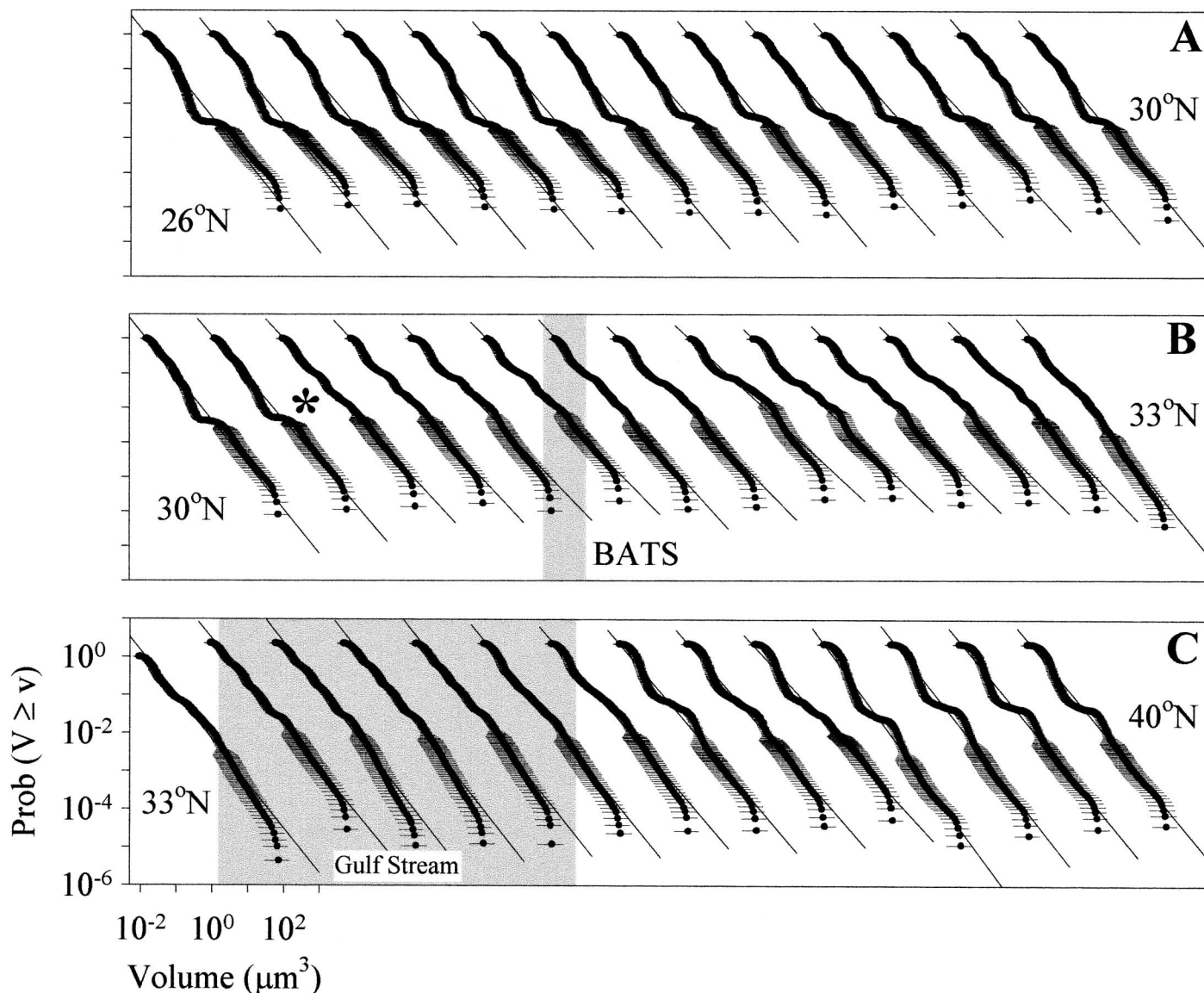


Fig. 4. Individual $\text{Prob}(V \geq v)$ size spectra for the transect. Spacing between spectra is constant in the figure but was not constant along transect (see Figs. 1, 3 for approximate spacing). Each panel represents a portion of the transect, with beginning and ending latitudes shown. Approximate locations of the BATS site and the Gulf Stream are indicated. An asterisk is added to B at the point separating southern and northern Sargasso Sea waters (see text).

nanoplankton group (arrow in Fig. 5F), whereas in the Gulf Stream, the gap is filled by a broadening of the size distributions of both the *Synechococcus* and ultra-nanoplankton groups (Fig. 5G). Thus, distinctly different communities yield very similar spectra. Gin (1996) found similar behavior, with bacteria filling the size occupied by *Prochlorococcus* when the latter were absent in coastal waters off Massachusetts. In the coastal spectra, *Prochlorococcus* are absent, causing a flattening in this part of the curve (Fig. 5D,H). Although there appears to be partial compensation for this by a broadening of the bacterial distribution, which was also observed by Gin (1996), it is not enough to smooth this part of the spectrum.

Theoretical models of size spectra (e.g., Kerr 1974; Sheldon et al. 1977; Platt and Denman 1978) have assumed

steady-state conditions for log-linear spectra, and deviations from linearity are sometimes explained as deviations from steady-state conditions (Sprules and Munawar 1986; Tittel et al. 1998). It is likely, however, that such deviations are also related to a fundamental ecosystem function (Warwick and Joint 1987). Consistent with this interpretation are reports of relatively uniform spectra seen in the stable central gyres of the oceans (Sheldon et al. 1972; Rodriguez and Mullin 1986), compared with nonlinear shapes found in dynamic high-latitude and coastal marine waters (Sheldon et al. 1972; Witek and Krajewska-Soltys 1989). It is noteworthy in this context that network models of ecological interactions of the type involved in marine communities are known to reach power-law distributions of size classes only asymptotically as time approaches infinity (Bonabeau et al.

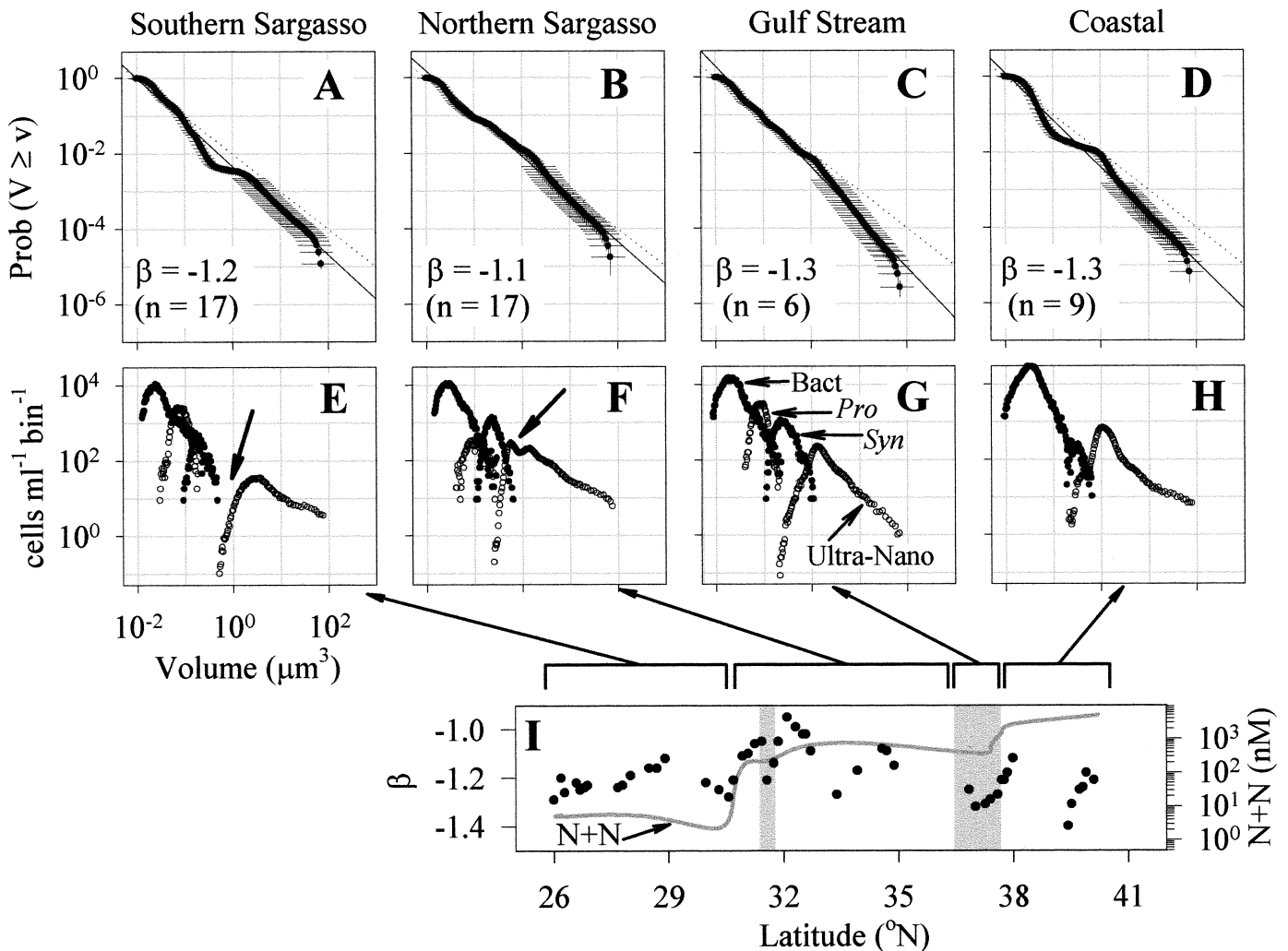


Fig. 5. Aspects of size spectra along March 1998 transect. (A–D) Ensemble averages of the probability of exceedence spectra, for (A) the southern Sargasso Sea, (B) the northern Sargasso Sea, (C) the Gulf Stream, and (D) coastal waters. Axes on the spectra plots, $\text{Prob}(V \geq v)$ and volume, are scaled the same for all panels, and slopes (β) of the regression lines (solid) are shown. Confidence intervals on the estimation of cell size are shown by horizontal lines for each point; variation among spectra are shown by vertical error bars (± 1 SD). In all cases, a 1-to-1 dotted line ($\beta = -1$) is included that begins at the volume of the smallest cell measured. (E–H) Representative plots of cell concentration against volume for the regions in (A–D). Four groups are shown (and denoted in panel G) from small to large: (i) heterotrophic bacteria, (ii) *Prochlorococcus*, (iii) *Synechococcus*, and (iv) the ultra- and nanoplankton. Arrows added to D and F to denote the absence of cells in these size classes for D and how this gap was filled by a subpopulation of the ultra- and nanoplankton that appeared in spring bloom waters for F (see text). (I) The slope (β) of the $\text{Prob}(V \geq v)$ spectra along the transect, with the smoothed fit for N+N from Fig. 3B added (note: shaded regions represent the approximate location of BATS and the Gulf Stream).

1999). Since we are not looking at the complete phytoplanktonic spectrum along the transect, and the larger sizes are likely to be more dynamic (Chisholm 1992), interpretations of the meaning of the nonlinear spectra in our data set would be highly speculative.

Spectral slope: The correlation coefficients (R^2) for the spectra varied only a small amount along the entire transect (range 0.96–0.99; data not shown). However, slopes (β) of individual spectra from the transect varied between -1.4 and -1.0 (Fig. 5I). The difference between slopes for groups of spectra was analyzed statistically by use of a nonparametric rank-sum test (two-tailed Mann–Whitney U test), following the approach used by others (Rodríguez and Mullin 1986;

Tittel et al. 1998). This tests for differences in β values between regions, based on their rank order, at the $P < 0.05$ level. Although there were significant changes in β across regions of the transect (Fig. 5I), the rank order of the β values shows that, overall, there was no relationship between β and nutrient concentrations. The region with the steepest slopes was the Gulf Stream. Next came the southern Sargasso, followed by the northern Sargasso. Slopes in coastal waters could not be distinguished ($P > 0.05$) from those in either the Gulf Stream or the southern Sargasso, but they were significantly steeper than in the northern Sargasso.

Formalizing the above observations, we found positive correlations between β and both N+N and SRP in the Sargasso Sea (Fig. 6A,C; $P < 0.01$). Also, as mentioned above,

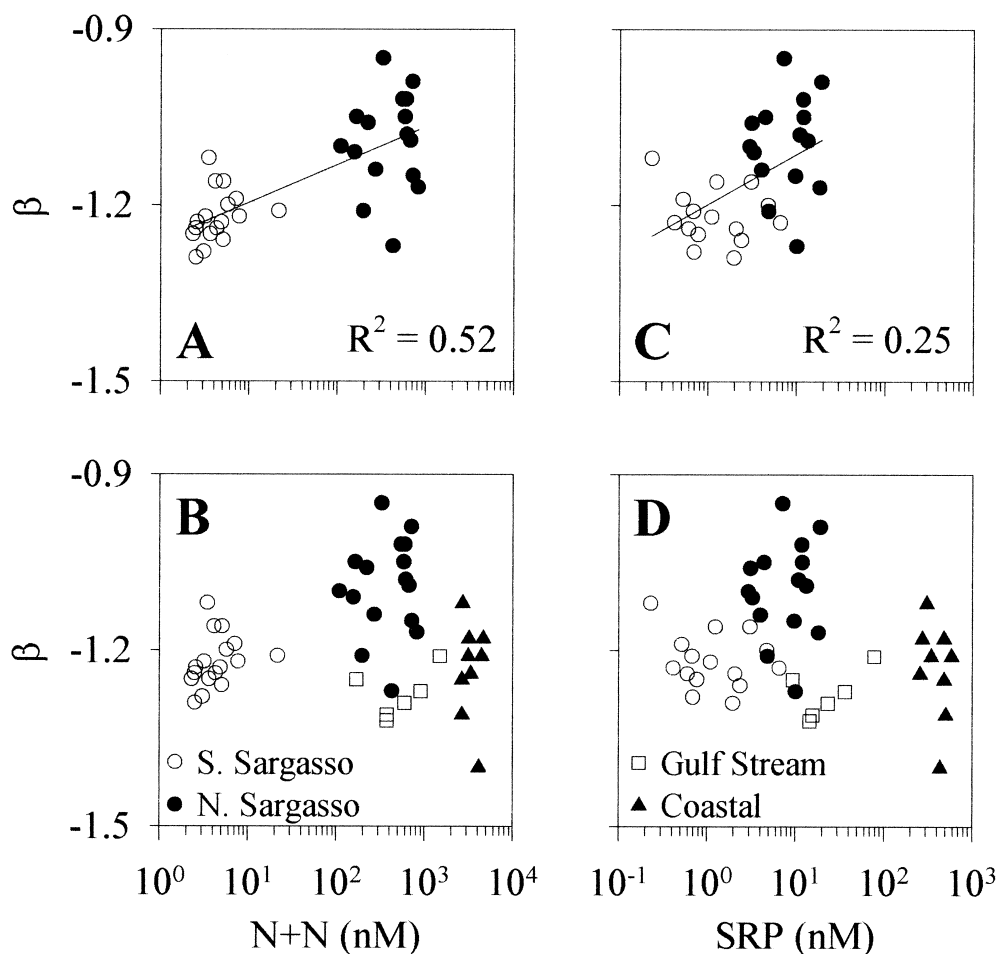


Fig. 6. Relationships between slope of the $\text{Prob}(V \geq v)$ plots (β) and (A,B) $N+N$ and (C,D) SRP. Regions of transect are indicated by different symbols shown in B and D for the southern Sargasso Sea, the northern Sargasso Sea, the Gulf Stream, and coastal waters.

there was an isolated correlation between β and nutrients at the northern edge of the Gulf Stream (Figs. 3B, 5I), where slopes became steadily less negative as nutrients increased sharply. It is generally believed that large cells, especially diatoms, predominate in nutrient-rich conditions (e.g., Chisholm 1992; Kiørboe 1993), which would give rise to less negative β values with increasing nutrients—just what was seen for the Sargasso Sea (Fig. 6A,C). As was indicated earlier, however, similar relationships between β and these two nutrient pools were not found across the entire data set (Fig. 6B,D). This may be due to the fact that a significant fraction of the larger cells that bloom in high nutrient conditions would have been out of our range of measurements; their inclusion might have flattened slopes. Another possible explanation for the lack of a universal relationship between β and nutrients might have been that heterotrophic bacteria probably respond to high nutrient conditions differently than do phytoplankton. In order to ensure that their inclusion in the spectra did not mask a relationship between β and nutrients for just the phytoplankton, we verified that the relationships in Fig. 6 were no more significant when bacteria were removed from the analyses (data not shown).

The overall ensemble spectrum: In order to look at the features of the entire data set, we ensemble-averaged the spectra shown in Fig. 4 into one single spectrum, treating the data as if all realizations (i.e., the individual spectra) could be interpreted as belonging to an identical statistical population (Fig. 7A). The ensemble spectrum adheres quite well to a smooth power-law distribution with a slope of -1.2 . We wondered whether this spectrum might more closely approach a slope of -1.0 , in which total biomass is equally distributed among all size classes, if we had been able to include microzooplankton in our measurements. Thus, we consulted published data to help us make some approximations. Caron et al. (1999) recently published representative size distributions for heterotrophic nanoplankton for a station close to the BATS site during both March–April and August. We added their August distribution to a sample from the well-stratified waters of the southern Sargasso (Fig. 7B) and added their March–April distribution to a sample from the high-nutrient waters near BATS (Fig. 7C). Quite remarkably, we found that the inclusion of microzooplankton to our spectra, which should approximate the full suite of plankton found in the size range studied, flattened the slope

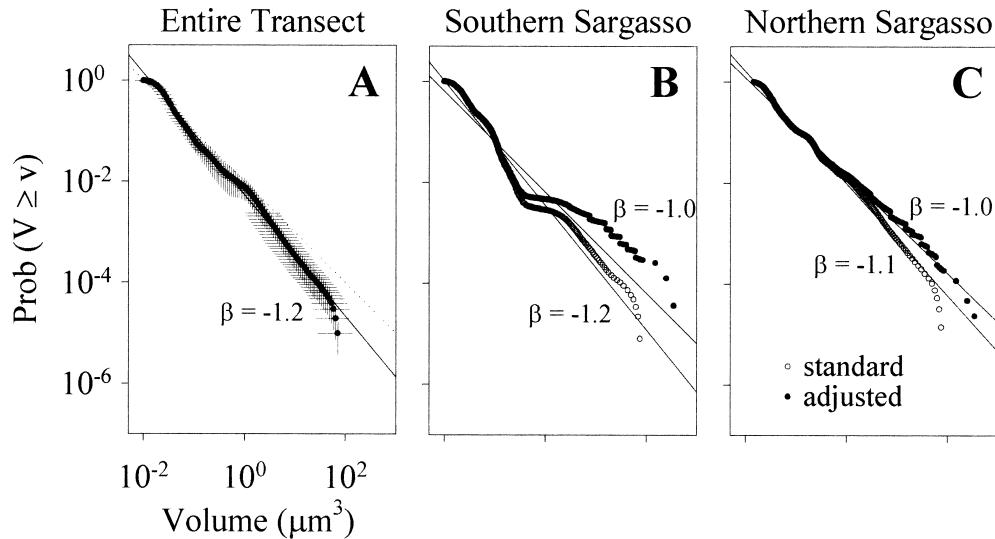


Fig. 7. Ensemble average spectra. (A) Individual spectra from all regions of the transect were averaged together (to weigh the four regions equally, similar numbers of spectra from each region were used). Estimated zooplankton biomass were added into spectra from the southern Sargasso (B) and northern Sargasso (C) (see text for details). See Fig. 5 legend for further details of plots.

to near the value $\beta = -1.0$ (Fig. 7B,C). Although this could be coincidental, it is consistent with the notion that, on average, there is a tendency toward a uniform distribution of biomass among size classes in pelagic ecosystems (Sheldon et al. 1972, 1977; Rodriguez and Mullin 1986).

Transient nutrient enrichment experiments

Our observations of spectra along the transect showed smooth power-law behavior in some cases, whereas, in others, certain size classes were under- or overrepresented relative to the regression line. We hypothesize that these discontinuities represent transients in the assembly of the food web, which, given ample—perhaps infinite—time, would ultimately disappear. Because it would be impossible to do the experiment necessary to test this hypothesis (i.e., to let these communities evolve undisturbed and see whether they settle into smooth power-law configurations), we did the inverse experiment and asked the question, what happens to the shapes of the spectra when a community is perturbed by an influx of nutrients? As mentioned above, the experimental design is somewhat flawed in that we are not measuring the large end of the phytoplankton spectrum, which is likely to be the most responsive in terms of biomass increase to nutrient enrichment. But in the context of this study, it is still of interest to see what happens to the small end of the spectrum in response to this sudden enrichment, as it is connected to the entire spectrum through food web dynamics. In addition, the pennate diatom population characterized by flow cytometry represented a large portion of the diatom community over roughly the first week of the iron-enrichment study (Cavender-Bares et al. 1999). We expected that species succession during such experiments would be manifested as multiple departures from a power law in the size spectrum, as has been observed during natural injections of

nutrients in coastal waters of the Mediterranean (Rodriguez et al. 1987).

Sargasso Sea enrichment experiment—The first experiment was conducted with nutrient-enriched communities enclosed in bottles at an oligotrophic station in the Sargasso Sea during June 1996 (Fig. 1). *Prochlorococcus* had extremely low abundances at the surface at this station, as is typical for the region in summer. Thus, the smallest size class of autotrophs was filled by *Synechococcus* throughout the experiment. Total Chl *a* increased >30-fold in bottles after N and P were added (Fig. 8A). Data from size-fractionated chlorophyll analyses indicated that ~75% of the total Chl *a* was in the <10 μm fraction—the fraction that approximates the size of cells observed by our flow cytometric method (data not shown). Thus, the majority of the total Chl *a* increase was due to the dramatic increases in *Synechococcus* and the ultra- and nanoplankton (Fig. 8B). In addition, bacteria doubled in abundance over the course of the incubation (Fig. 8B).

The spectra describing the initial community for this experiment followed the general power-law pattern, with a slope of -1.1 (Fig. 8C). Over the 5 d of the experiment in control bottles, the slope steepened to -1.2 as a result of slight relative increases in the concentration of the two smallest groups: bacteria and *Synechococcus*. In clear contrast, the slope of the spectra from the nutrient-enriched bottles became flatter with time, reflecting blooms of *Synechococcus*, which also happened to grow larger in size, and the ultra- and nanoplankton (Fig. 8D). Slopes from the two treatments differed by 0.2 units on day 5, indicating that relatively more of the total biovolume was contained within cells of large size in the bottles amended with N and P than that in control bottles.

The *Synechococcus* cells that bloomed in the enriched bottles also became larger, which is evident by the plateau in

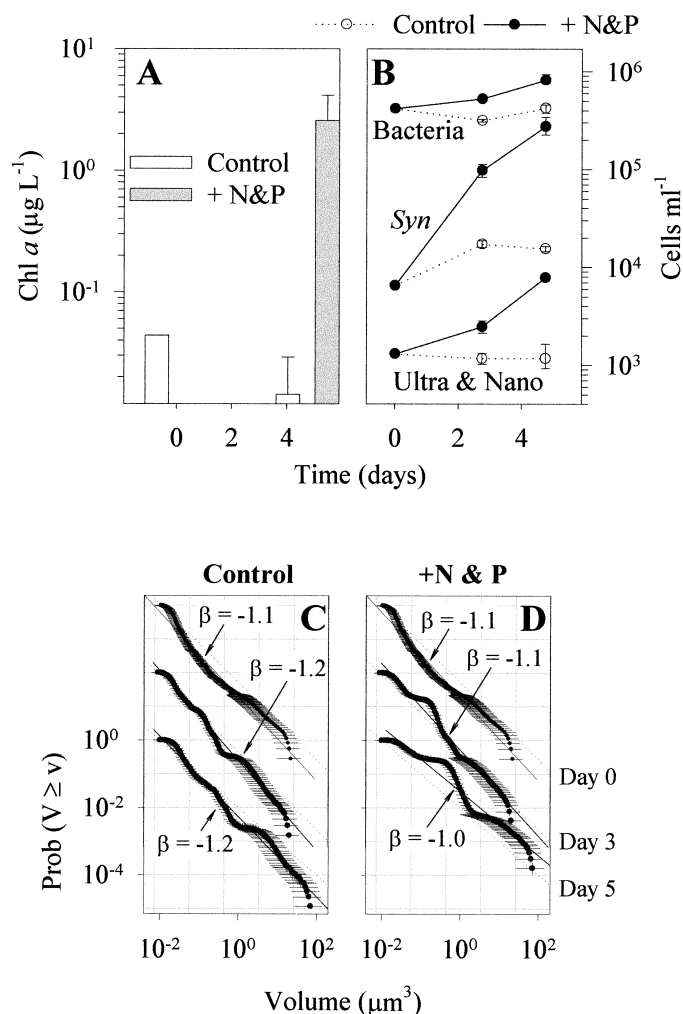


Fig. 8. Size spectra from a nutrient enrichment experiment in the Sargasso Sea (Fig. 1). (A) Endpoint Chl *a* from duplicate bottles. (B) Changes in cell concentration for three microbial groups ordered from small to large cell size: bacteria, *Synechococcus*, and the ultra- and nanophytoplankton (see text for further descriptions). (C,D) Size spectra from three sampling times (days 0, 3, and 5) for control bottles (C) and bottles with added NO_3 and PO_4 (+N and P; D). Note that the spectrum for day 0 is repeated in both panels. Each spectrum represents the average for triplicate bottles, with vertical error bars indicating the range between replicates. Spectra for a given day have been offset vertically so that they are easily compared. The offset is equivalent to three orders of magnitude between each successive day. See Fig. 5 legend for further details of plots.

the spectra centered at $\sim 0.1 \mu\text{m}^3$ (i.e., *Synechococcus* moved out of those size classes, resulting in a size gap that apparently was not filled by other groups). The huge numbers of *Synechococcus* translated into a rapidly declining probability of exceedence curve between the plateau and slightly beyond $1 \mu\text{m}^3$. The bloom of the ultra- and nanophytoplankton resulted in a similar feature between 1 and $10 \mu\text{m}^3$.

IronEx II study in the equatorial Pacific—Our second nutrient perturbation study comes from an in situ iron enrichment experiment conducted in the equatorial Pacific (IronEx II; Coale et al. 1996), in which “bottle effects” were elim-

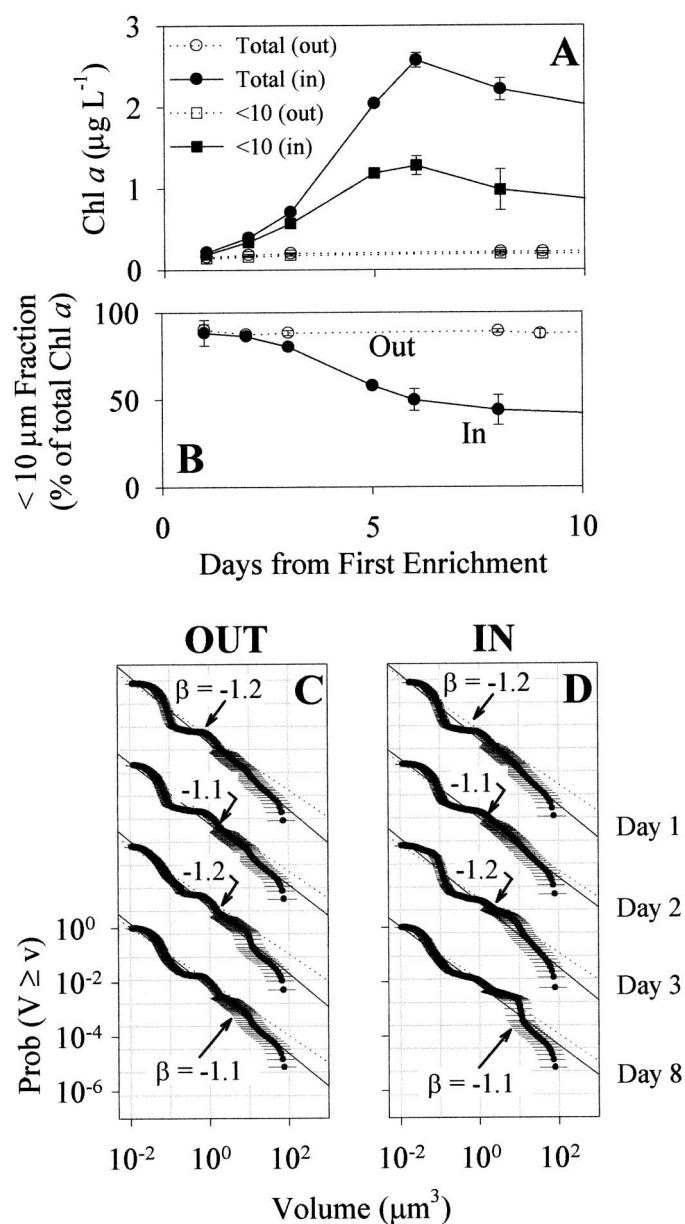


Fig. 9. Size spectra from the IronEx II study in the equatorial Pacific Ocean during May and June 1995. (A) Changes in the total and the $<10 \mu\text{m}$ fraction of Chl *a* with time outside and inside the iron-enriched patch (adapted from Cavender-Bares et al. 1999) (B) Percentage of the total Chl *a* found in the $<10 \mu\text{m}$ fraction. (C,D) Two spectra are shown for each day representing stations outside (C) and inside (D) iron-enriched waters. For details of spectral plots, see Figs. 5 and 8 legends.

inated. That is, the entire food web remained intact during the experiment. Our previous reports on the community response during IronEx II showed that all phytoplankton groups were stimulated by the addition of iron, but only the pennate diatoms and other large-sized diatoms increased in numbers dramatically relative to control waters outside the enriched patch (Cavender-Bares et al. 1999). This response can be summarized by the >10 -fold increase in Chl *a* over the first 6 d of the experiment (Fig. 9A; Cavender-Bares et

al. 1999) and a drop in the contribution of the $<10 \mu\text{m}$ size fraction to total chlorophyll (Fig. 9A,B).

Despite these dramatic changes in the *total* phytoplankton community in response to iron enrichment, values of β , for spectra that included only the small end of the phytoplankton community and the bacteria, differed little for samples taken from outside or inside fertilized waters over the course of the experiment (Fig. 9C,D). The spectral shapes both before and after iron enrichment were distinctly not log linear, and, although there were some differences between the enriched and unenriched communities, their general features were remarkably similar. The documented bloom of pennate diatoms (Coale et al. 1996; Cavender-Bares et al. 1999), which *can* be seen in the shape of the spectra on day 8, is a notable exception (Fig. 9D).

Overall, differences between the control and nutrient-enriched spectra for the subset of the community we measured were less dramatic in the IronEx II experiment than those in the Sargasso Sea bottle experiments. Although pure speculation, this may result from the fact that a fully represented grazing community was present in the IronEx II study in comparison to the bottle incubations in the Sargasso Sea, where grazers—both micro and macro—should have been underrepresented because of “bottle effects.” If true, this would imply that, when the full food web is functioning, the spectra tend more toward a power-law shape than when the flow of energy through the system is constrained by bottle effects.

Conclusions and speculations

We have studied the size spectra of microbial plankton sampled from a transect in the western north Atlantic Ocean and compared them with spectra derived from experiments involving nutrient manipulations. The most noteworthy conclusions are (1) the variability among spectra within each of the four regions studied was small, suggesting that they represent a conservative feature of the food web over large regions of the oceans; and (2) the ensemble average of all the spectra revealed that variability among different community size distributions was also small. As have others before us (e.g., Rodriguez and Mullin 1986), we find this constancy remarkable.

Although we are looking at only a small fraction of the planktonic size spectrum in our analysis, the fact that the ensemble spectrum obeys a power law invites some speculation. Power laws are characteristic of scale-free distributions (i.e., where the mean size of a sample depends on the range of sizes resolved). If that is the case, as Sheldon et al. (1972) noted, the very definition of mean phytoplankton size becomes meaningless. In turn, a power law decay of probability of a geometric attribute like size implies scale invariance, which is a property commonly attributed to the geometry of nature, and a continuum of scales (i.e., all sizes appearing in the spectrum without one size being more characteristic than others—e.g., Schroeder 1991). A scale-invariant distribution would call for a tendency of planktonic ecosystems to self-organize into a critical state without a characteristic size, regardless of initial states or any disorder

affecting the ecosystem. This complies with the basic mechanisms of self-organization of several open, dissipative systems with many degrees of freedom (Bak 1996).

Clearly, this study poses more questions than it answers regarding the underlying mechanisms dictating pelagic size spectra. We do think, however, that the clear power-law behavior of the spectra in certain regions begs for an explanation. We tentatively hypothesize that the wavy distributions seen in some cases represent transients, whereas those displaying algebraic decay represent systems under optimum conditions. Power-law behavior can be an important dynamic indicator, and it behooves us to seek similarities between the planktonic systems and other systems that display such scale-invariant behavior.

References

- ACKELSON, S. G., AND R. W. SPINRAD. 1988. Size and refractive index of individual marine particulates: A flow cytometric approach. *Appl. Optics* **27**: 1270–1277.
- AHRENS, M. A., AND R. H. PETERS. 1991. Patterns and limitations in limnoplankton size spectra. *Can. J. Fish. Aquat. Sci.* **48**: 1967–1978.
- ALBERT, R., H. JEONG, AND A. L. BARABASI. 2000. Error and attack tolerance of complex networks. *Nature* **406**: 378–382.
- ARMSTRONG, R. A. 1999. Stable model structures for representing biogeochemical diversity and size spectra in plankton communities. *J. Plankton Res.* **21**: 445–464.
- BADER, H. 1970. The hyperbolic distribution of particle sizes. *J. Geophys. Res.* **75**: 2822–2830.
- BAK, P. 1996. How nature works: The science of self-organized criticality. Copernicus-Springer.
- BARABASI, A. L., AND R. ALBERT. 1999. Emergence of scaling in random networks. *Science* **286**: 509–512.
- BLANCO, J. M., F. ECHEVARRÍA, AND C. M. GARCÍA. 1994. Dealing with size-spectra: Some conceptual and mathematical problems. *Sci. Mar.* **58**: 17–29.
- BOHREN, C. F., AND D. R. HUFFMAN. 1983. Absorption and scattering of light by small particles. Wiley.
- BONABEAU, E., L. DAGORN, AND P. FRÉON. 1999. Scaling in animal group-size distributions. *Proc. Natl. Acad. Sci. USA* **96**: 4472–4477.
- CARON, D. A., E. R. PEELE, E. L. LIM, AND M. R. DENNETT. 1999. Picoplankton and nanoplankton and their trophic coupling in surface waters of the Sargasso Sea south of Bermuda. *Limnol. Oceanogr.* **44**: 259–272.
- CAVENDER-BARES, K. K. 1999. Size distributions, population dynamics, and single-cell properties of marine plankton in diverse nutrient environments. Ph.D. thesis, Massachusetts Institute of Technology.
- , S. L. FRANKEL, AND S. W. CHISHOLM. 1998. A dual sheath flow cytometer for shipboard analyses of phytoplankton communities from the oligotrophic oceans. *Limnol. Oceanogr.* **43**: 1383–1388.
- , D. M. KARL, AND ———. In press. Nutrient gradients in the western North Atlantic Ocean: Relationship to microbial community structure, and comparison to patterns in the Pacific Ocean. *Deep-Sea Res.*
- , E. L. MANN, S. W. CHISHOLM, M. E. ONDRUSEK, AND R. R. BIDIGARE. 1999. Differential response of equatorial Pacific phytoplankton to iron fertilization. *Limnol. Oceanogr.* **44**: 237–246.
- CHISHOLM, S. W. 1992. Phytoplankton size, p. 213–237. *In* P. G.

- Falkowski and A. D. Woodhead [eds.], Primary productivity and biogeochemical cycles in the sea. Plenum.
- COALE, K. H., AND OTHERS. 1996. A massive phytoplankton bloom induced by an ecosystem-scale iron fertilization experiment in the equatorial Pacific Ocean. *Nature* **383**: 495–501.
- DUGDALE, R. C., AND J. J. GOERING. 1967. Uptake of new and regenerated forms of nitrogen in primary productivity. *Limnol. Oceanogr.* **12**: 196–206.
- FANNING, K. A. 1992. Nutrient provinces in the sea: Concentration ratios, reaction rate ratios, and ideal convariation. *J. Geophys. Res.* **97**: 5693–5712.
- GAEDKE, U. 1992. The size distribution of plankton biomass in a large lake and its seasonal variability. *Limnol. Oceanogr.* **37**: 1202–1220.
- GARSDALE, C. 1982. A chemiluminescent technique for the determination of nanomolar concentrations of nitrate and nitrite in seawater. *Mar. Chem.* **11**: 159–167.
- GIN, K. 1996. Microbial size spectra from diverse marine ecosystems. Ph.D. thesis, Massachusetts Institute of Technology and Woods Hole Oceanographic Institute.
- , S. W. CHISHOLM, AND R. J. OLSON. 1999. Seasonal and depth variation in microbial size spectra at the Bermuda Atlantic time series station. *Deep-Sea Res.* **46**: 1221–1245.
- , J. GUO, AND H.-F. CHEONG. 1998. A size-based ecosystem model for pelagic waters. *Ecol. Model.* **112**: 53–72.
- HOLLING, C. S. 1992. Cross-scale morphology, geometry, and dynamics of ecosystems. *Ecol. Monogr.* **62**: 447–502.
- KARL, D. M., AND G. TIEN. 1992. MAGIC: A sensitive and precise method for measuring dissolved phosphorus in aquatic environments. *Limnol. Oceanogr.* **37**: 105–116.
- KERR, S. R. 1974. Theory of size distribution in ecological communities. *J. Fish. Res. Board Can.* **31**: 1859–1862.
- KIEFER, D. A., AND J. BERWALD. 1992. A random encounter model for the microbial planktonic community. *Limnol. Oceanogr.* **37**: 457–467.
- KIØRBOE, T. 1993. Turbulence, phytoplankton cell-size, and the structure of pelagic food webs. In J. H. S. Blaxter and A. J. Southward [eds.], *Advances in marine biology*, v. 29. Academic.
- LEPESTEUR, M., J. M. MARTIN, AND A. FLEURY. 1993. A comparative-study of different preservation methods for phytoplankton cell analysis by flow-cytometry. *Mar. Ecol. Prog. Ser.* **93**: 55–63.
- LI, W. K. W. 1994. Phytoplankton biomass and chlorophyll concentration across the North Atlantic. *Sci. Mar.* **58**: 67–79.
- MANDELBROT, B. B. 1983. The fractal geometry of nature. Freeman.
- MARIE, D., F. PARTENSKY, S. JACQUET, AND D. VAULOT. 1997. Enumeration and cell cycle analysis of natural populations of marine picoplankton by flow cytometry using the nucleic acid stain SYBR Green I. *Appl. Environ. Microbiol.* **63**: 186–193.
- MICHAELS, A. F., AND OTHERS. 1994. Seasonal patterns of ocean biogeochemistry at the U.S. JGOFS Bermuda Atlantic Time-series Study site. *Deep-Sea Res.* **41**: 1013–1038.
- OLSON, R. J., E. R. ZETTLER, AND O. K. ANDERSON. 1989. Discrimination of eukaryotic phytoplankton cell-types from light scatter and autofluorescence properties measured by flow-cytometry. *Cytometry* **10**: 636–643.
- PLATT, T. 1985. Structure of the marine ecosystem: Its allometric basis. *Can. J. Fish. Aquat. Sci.* **213**: 55–64.
- , AND K. L. DENMAN. 1978. The structure of pelagic marine ecosystems. *Rapp. P.-V. Réun. Cons. Int. Explor. Mer* **173**: 60–65.
- PROTHERO, J. 1986. Methodological aspects of scaling in biology. *J. Theor. Biol.* **118**: 259–286.
- ROBERTSON, B. R., D. K. BUTTON, AND A. L. KOCH. 1998. Determination of the biomasses of small bacteria at low concentrations in a mixture of species with forward light scatter measurements by flow cytometry. *Appl. Environ. Microbiol.* **64**: 3900–3909.
- RODRIGUEZ, J., F. JIMÉNEZ, B. BAUTISTA, AND V. RODRIGUEZ. 1987. Planktonic biomass spectra dynamics during a winter production pulse in Mediterranean coastal waters. *J. Plankton Res.* **9**: 1183–1194.
- , AND M. M. MULLIN. 1986. Relation between biomass and body weight of plankton in a steady-state oceanic ecosystem. *Limnol. Oceanogr.* **31**: 316–370.
- RUIZ, J., C. M. GARCÍA, AND J. RODRÍGUEZ. 1996. Vertical patterns of phytoplankton size distribution in the Cantabric and Balearic Seas. *J. Mar. Syst.* **9**: 269–282.
- SCHROEDER, M. R. 1991. Fractals, chaos, and power-laws: minutes from an infinite universe. Freeman.
- SHELDON, R. W., AND T. R. PARSONS. 1967. A continuous size spectrum for particulate matter in the sea. *J. Fish. Res. Board Can.* **24**: 909–915.
- , A. PRAKASH, AND W. H. SUTCLIFFE. 1972. The size distribution of particles in the ocean. *Limnol. Oceanogr.* **17**: 327–340.
- , W. H. SUTCLIFFE, JR., AND M. A. PARANJAE. 1977. Structure of pelagic food chain and relationship between plankton and fish production. *J. Fish. Res. Board Can.* **34**: 2344–2353.
- SPRULES, W. G., J. M. CASSELMAN, AND B. J. SHUTER. 1983. Size distribution of pelagic particles in lakes. *Can. J. Fish. Aquat. Sci.* **40**: 1761–1769.
- , AND M. MUNAWAR. 1986. Plankton size spectra in relation to ecosystem productivity, size, and perturbation. *Can. J. Fish. Aquat. Sci.* **43**: 1789–1794.
- STRAMSKI, D., AND D. A. KIEFER. 1991. Light scattering by microorganisms in the open ocean. *Prog. Oceanogr.* **28**: 343–383.
- TITTEL, J., B. ZIPPEL, W. GELLER, AND J. SEEGER. 1998. Relationships between plankton community structure and plankton size distribution in lakes of northern Germany. *Limnol. Oceanogr.* **43**: 1119–1132.
- VIDONDO, B., Y. T. PRAIRIE, J. M. BLANCO, AND C. M. DUARTE. 1997. Some aspects of the analysis of size spectra in aquatic ecology. *Limnol. Oceanogr.* **42**: 184–192.
- WARWICK, R. M., AND I. R. JOINT. 1987. The size distribution of organisms in the Celtic Sea: From bacteria to Metazoa. *Oecologia* **73**: 185–191.
- WELSCHMEYER, N. A. 1994. Fluorometric analysis of chlorophyll *a* in the presence of chlorophyll *b* and pheopigments. *Limnol. Oceanogr.* **39**: 1985–1992.
- WITEK, Z., AND A. KRAJEWSKA-SOLTYS. 1989. Some examples of the epipelagic plankton size structure in high latitude oceans. *J. Plankton Res.* **11**: 1143–1155.
- WU, J. F., W. SUNDA, AND E. A. BOYLE. 2000. Phosphate depletion in the western North Atlantic Ocean. *Science* **289**: 759–762.
- YENTSCH, C. S., AND D. A. PHINNEY. 1989. A bridge between ocean optics and microbial ecology. *Limnol. Oceanogr.* **34**: 1694–1705.

Received: 15 February 2000

Accepted: 23 November 2000

Amended: 30 January 2001